

Alveolar Echinococcosis of the Liver: MR Findings

Michel Claudon, Michel Bessieres, Denis Regent, Alain Rodde, Christophe Bazin,
Alain Gerard, and Laurent Bresler

Abstract: Nineteen cases of proven hepatic alveolar echinococcosis were examined by magnetic resonance (MR) and the results were compared with CT. Fibrous and parasitic tissue showed low signal both on T1- and, generally, on T2-weighted images. In a few cases a high signal on T2-weighted images may be observed, due either to central necrotic zones or to small peripheral cysts. Central necrosis was more easily identified by MR than by CT. However, MR seemed to be less effective than CT in allowing us to reach a positive diagnosis, due to its inability to show microcalcifications. In addition, MR may not reveal small lesions. In most cases T1-weighted images revealed more clearly than CT did the margins of the lesions and the hepatic extension, especially to hepatic veins, vena cava, and perihepatic spaces. **Index Terms:** Liver, diseases—Parasites—Lungs, diseases—Computed tomography—Magnetic resonance imaging—Echinococcosis.

Alveolar echinococcosis (AE) is a rare parasitic disease due to the intrahepatic growth of the larva of *Echinococcus multilocularis*. The disease is usually found in central Europe, the Soviet Union, Japan, and North America (1–5). Humans can be accidentally contaminated by ingestion of infected berries or plants or by direct contact with foxes, which are usually the main hosts of the parasitic cycle. In contrast to *E. granulosus*, *E. multilocularis* grows with external vesiculation, surrounded by a fibroinflammatory reaction; the result is an infiltrative tumor-like mass that very slowly invades the liver, especially the portal spaces and hilum, the hepatic veins, and the vena cava. Microcalcifications and central necrosis are frequent, due to vascular involvement and ischemia (6). Extrahepatic extension through the diaphragm or toward the duodenum and retroperitoneum is possible as are metastases to the lungs, brain, or bone (7).

At present, the treatment is controversial. Although medical therapy may stabilize the lesions in some cases (8), definitive cure can only be obtained by partial hepatectomy of localized masses or by orthotopic transplantation of the liver in advanced cases (2,9,10).

From the Service de Radiologie (M. Claudon, M. Bessieres, D. Regent, A. Rodde, and C. Bazin), Département des Maladies Infectieuses et Tropicales (A. Gerard), and Service de Chirurgie C (L. Bresler), Centre Hospitalier Universitaire de Nancy, 54511 Vandoeuvre, France. Address correspondence and reprint requests to Dr. M. Claudon.

Radiological methods play an important role in the initial evaluation of parasitic extension before a therapeutic decision is made as well as in the long-term follow-up of patients who are under medical therapy (1,3–5). In our institution CT and occasionally ultrasound are performed once a year or more often in the case of progression. However, MR may be a more precise method for the evaluation of liver masses. The aim of our study is to describe the MR patterns of AE, which to our knowledge have not been reported before, and to compare them with the respective CT data.

MATERIALS AND METHODS

During the period from May 1988 to February 1989, 19 patients (7 men and 12 women, 22–81 years of age, mean 59 years) with hepatic AE were examined by CT and MR. The diagnosis was confirmed in all cases by specific serology (enzyme-linked immunosorbent assay) and in eight cases by biopsy.

The diagnosis was recently established in four patients, whereas the other 15 patients have been followed for 1–7 years (mean 4.4 years), and all were treated with benzimidazoles. Among these 15, three had a right hepatectomy, one drainage of a cystic mass, and one a biliary-enteric anastomosis. The main clinical symptoms were hepatomegaly (eight cases); asthenia, abdominal pain, and fever (seven cases); and jaundice (four cases).

All patients were studied on a 0.5 T unit (Magniscan, CGR) with a body coil, a field of view of 40 cm, a matrix of 256×256 , and a slice thickness of 9 mm with a gap of 1–2 mm. Axial views were obtained in all cases. Sagittal or frontal views were obtained in case of extrahepatic extension.

The T1 weighting was achieved with a repetition time (TR) ranging from 360 to 700 ms and an echo time (TE) of 26 ms; T2 weighting was achieved with a TR of 2,000 ms and a TE of 50, 100, and 150 ms. Cardiac gating was used in cases of transdiaphragmatic extension.

Magnetic resonance and CT were performed during the same week. The MR images were reviewed to obtain a specific description and were then compared with the CT data.

The CT data were the basis for comparison in this study. The CT scanner was either Philips Tomoscan 350, a Siemens Somatom DRH, or a CGR CE 10000. Adjacent axial scans 9 or 10 mm thick were obtained before and after intravenous bolus contrast medium administration (sodium meglumine ioxithalamate, Telebrix, Guerbet).

Hepatomegaly was encountered in 10 cases, sometimes due to secondary hypertrophy of normal parenchyma, but more often due to the large volume of the lesions.

There was one lesion in 13 cases (size 1.5–25 cm,

mean 12.3 cm), two lesions in two cases, three in two cases, and five in one case (size 1.5–14 cm, mean 3.5 cm) (total number of lesions was 28). One other case was a miliary form with >20 foci (size, 1–3 cm). The right hepatic lobe was mainly involved in 11 cases and the left lobe in the other eight cases. An extension to the hilum was noted in 11 cases and to the hepatic vein convergence in seven cases. Extrahepatic involvement was found in three cases (one to pericardium; one with pulmonary, retroperitoneal, and lumbar spine extension; one metastatic to the thoracic spine). No lymphadenopathy was observed.

The parasitic tissue was of low density (30–40 HU) and easily recognized because of negligible enhancement after contrast medium injection, which therefore allowed a good delineation of the lesion's edges. Clusters of microcalcifications or large calcium deposits were encountered in 17 of the 28 lesions (61%) and central necrosis was encountered in 14 lesions (50%).

RESULTS

The following features were observed (Figs. 1–5): (a) Fibrous and parasitic tissue was shown as slightly inhomogeneous areas of low signal intensity

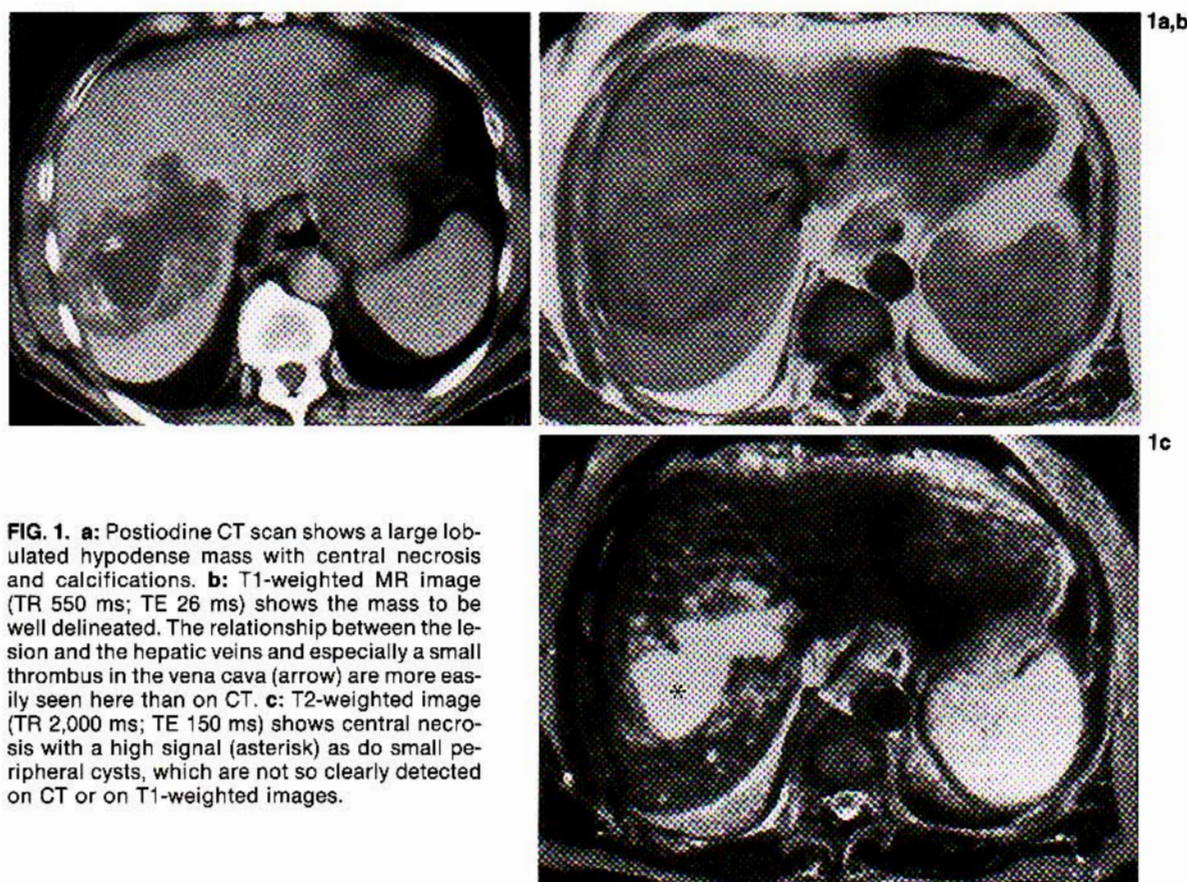


FIG. 1. a: Postiodine CT scan shows a large lobulated hypodense mass with central necrosis and calcifications. **b:** T1-weighted MR image (TR 550 ms; TE 26 ms) shows the mass to be well delineated. The relationship between the lesion and the hepatic veins and especially a small thrombus in the vena cava (arrow) are more easily seen here than on CT. **c:** T2-weighted image (TR 2,000 ms; TE 150 ms) shows central necrosis with a high signal (asterisk) as do small peripheral cysts, which are not so clearly detected on CT or on T1-weighted images.

on T1-weighted images in all cases. On strongly T1-weighted images (TR 300–400 ms) the contrast between the lesion and the adjacent liver was improved and the delineation of mass margins was easier. On T2-weighted images a very low signal intensity was observed in 15 cases, whereas in the other four cases a rather high signal intensity was noted, increasing on the first and second echo but decreasing on the third echo. In addition, in three cases small circular and peripheral (diameter ≤ 1 cm) areas of very high signal intensity were shown. (b) Necrosis was shown as areas of low signal intensity on T1-weighted images but very high signal intensity on T2-weighted images in 14 cases (50%). They were always central, sometimes lobulated, with irregular margins. In the case of massive necrosis the general pattern was a pseudocyst, surrounded by an irregular boundary of low signal intensity on T1-weighted images and low or intermediate signal intensity on T2-weighted images. (c) Calcifications were suspected in only four cases (18%) by MR. The largest calcium deposits were recognized within the parasitic tissue because of their very low signal on both T1- and T2-weighted

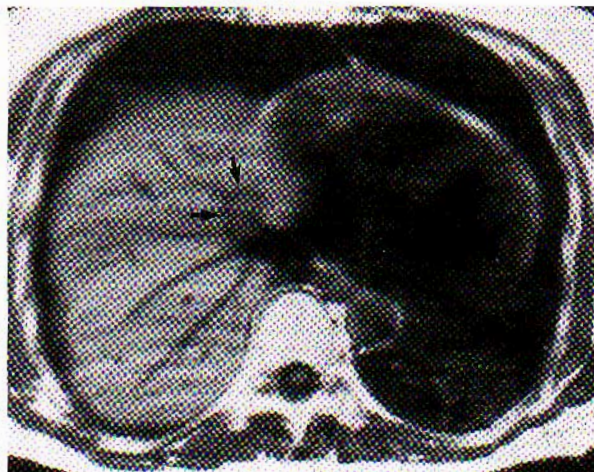
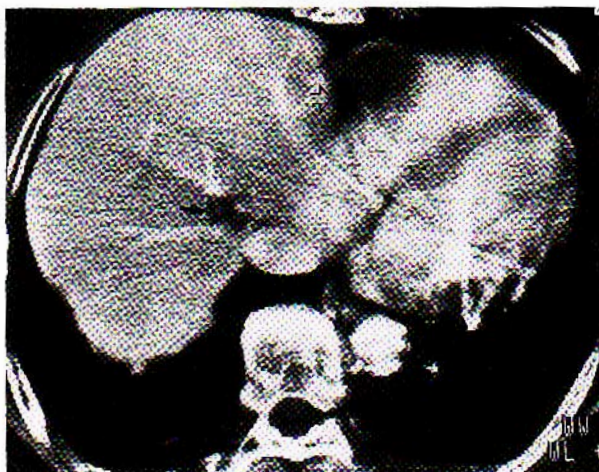
images. Small clusters of calcification were not observed.

The hepatic veins were always well observed up to the first-order branching, especially on T1-weighted images, because of an absence of signal due to flow phenomena. They were uninvolved in five cases; in 10 cases one or two veins were displaced by adjacent and/or large lesions but, nevertheless, remained patent. Obliteration was noted in four cases of large masses that involved an entire lobe of the liver. An extension to the convergence of the hepatic veins was observed in three cases, with evidence of a small cava thrombus in two of them (Figs. 1 and 2).

The retrohepatic vena cava was compressed by large, posterior masses in three cases, but the persistence of flow was easily shown (Figs. 3 and 6).

The portal veins were also clearly seen, especially in the right lobe: an analysis was more difficult in the left lobe because of artifacts due to breathing, image aliasing, or aortic flow phenomena. The segmental branches were uninvolved in nine cases; they were displaced but without obstruction in five cases. Thrombosis of the right

2a,b



2c

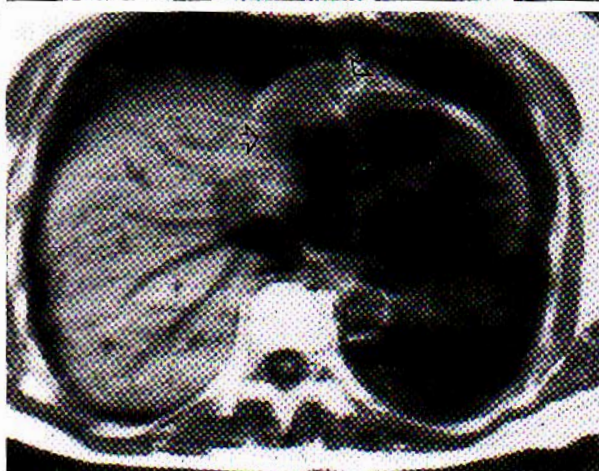


FIG. 2. a: Postiodine CT scan shows hypodense lesion near the hepatic veins (solid arrow) and a second close to the right cardiac ventricle (open arrow). b: Strongly T1-weighted image (TR 400 ms; TE 26 ms) clearly shows the first lesion and its proximity to the adjacent parenchyma and hepatic veins (arrows). c: T1-weighted image with cardiac gating clearly shows the second lesion and its cardiac extension (open arrows), but the first lesion cannot be clearly seen due to the prolonged TR during cardiac gating.

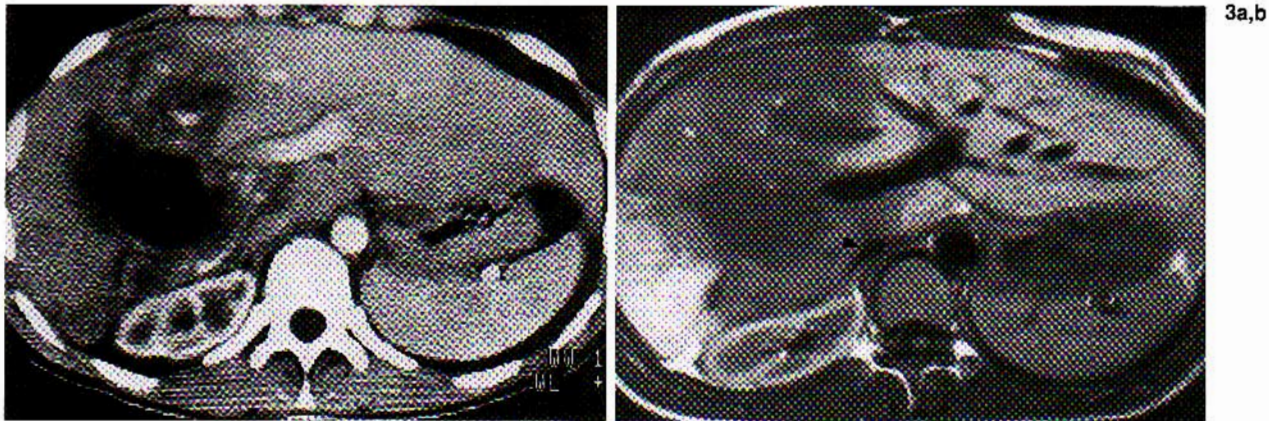


FIG. 3. **a:** Postiodine CT scan shows large calcified and necrotic mass in the right and medial segment of left lobes with obstruction of the right portal vein. **b:** T1-weighted MR image (TR 600 ms) shows the lesion edges as well as the extension to the portal vessels. The blood flow in the vena cava is unobstructed (arrowhead).

branches in three cases and of the left branches in two cases was suspected. Dilatation of the main segmental biliary ducts (four cases) was displayed only on T2-weighted images (Fig. 4). Extension of the parasitic mass through the diaphragm to the

pleura and lung or to the pericardium and heart was most easily seen on cardiac gated sequences (Fig. 2). Coronal and sagittal views were also useful in such cases as well as in the case of retroperitoneal extension (Fig. 6).

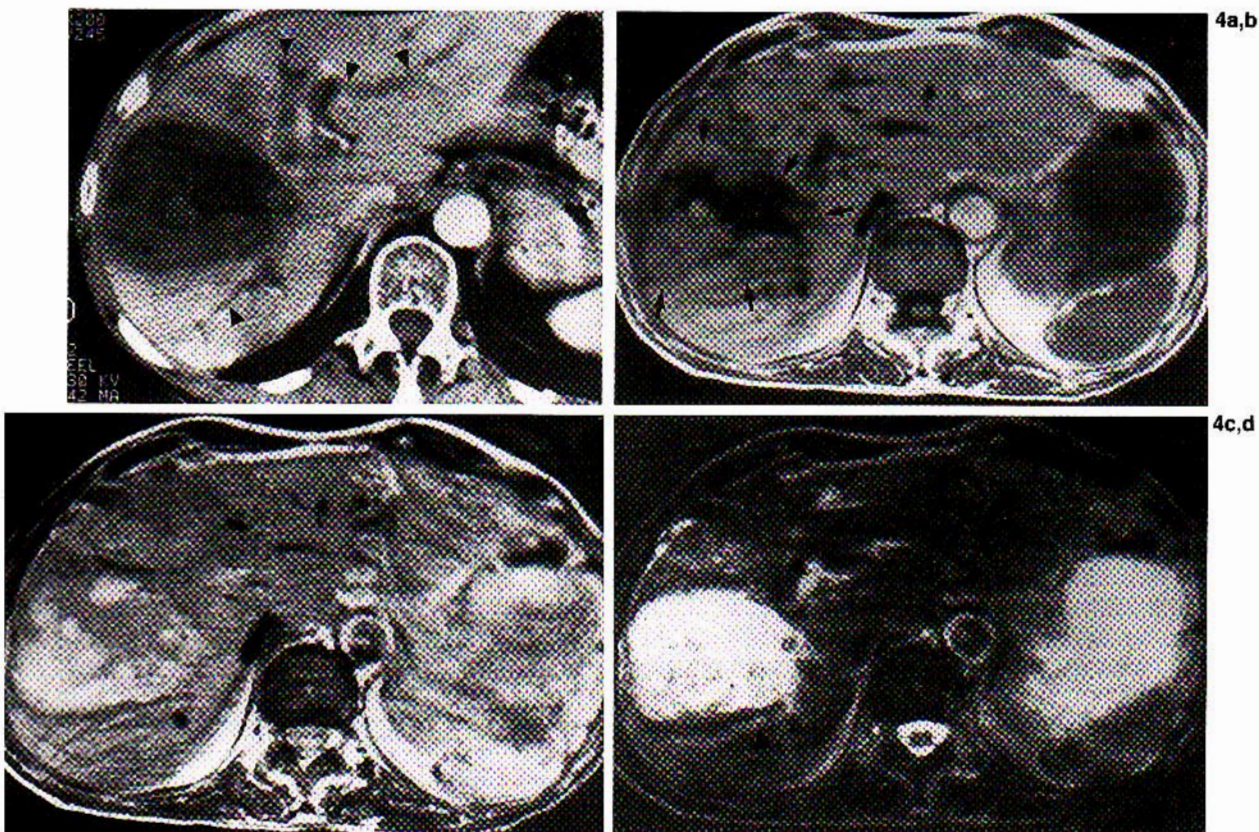


FIG. 4. Right necrotic mass involving the hilum. **a:** Postiodine CT scan shows large necrotic mass with biliary dilatation (arrowheads). **b:** T1-weighted MR image (TR 500 ms) shows central necrosis as an area of very low signal, surrounded by an irregular rim of low signal due to fibrous and parasitic tissue (arrows). **c** and **d:** T2-weighted images [TR 2,000 ms; TE 50 ms (c) and TE 150 ms (d)] show the peripheral fibrous and parasitic tissue to have a higher signal than the necrosis on the first echo (c) and a lower signal on the third echo (d). The biliary dilatation is visible on the third echo (arrowheads, d), but CT is more accurate.

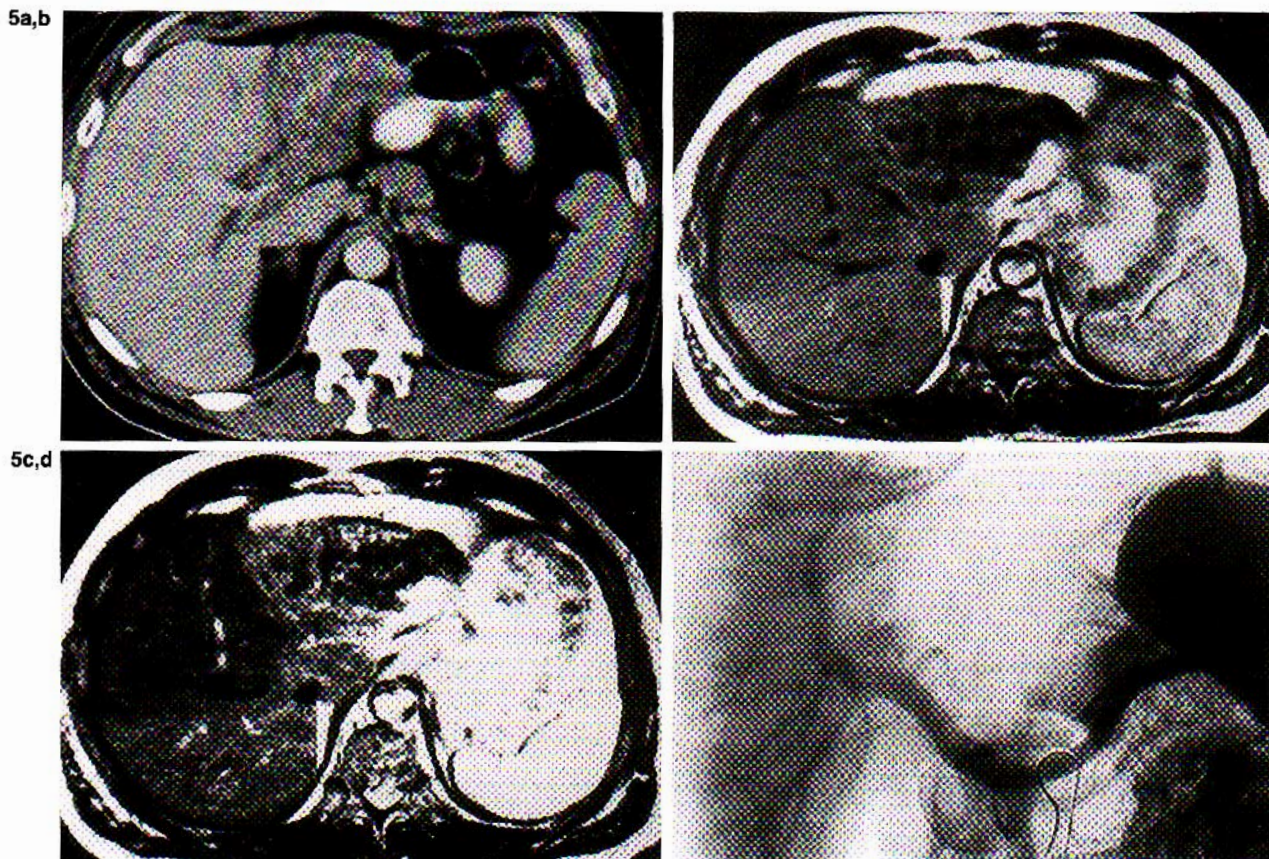


FIG. 5. CT scan (a) shows slightly calcified mass in left lobe involving the hilum. T1-weighted (b) (TR 550 ms; TE 26 ms) and T2-weighted (c) (2,000 ms; TE 150 ms) images show low, heterogeneous signal of the fibrous and parasitic mass; low signal in the anterior part and intermediate signal in the posterior part of the right hepatic lobe and caudate lobe. Angiography (d) (portal phase) demonstrates obstruction of the left branch, which explains the asymmetry of the MR signal in the right lobe.

Analysis of both T1- and T2-weighted images permitted the detection of 23 of 28 lesions already detected by CT in the first 18 patients. Five lesions of small size (<2 cm), easily shown in CT, were not recognized in the MR images. In one case the T1 lesion–liver contrast may have decreased due to the use of a relatively long TR (700 ms). Two other lesions were very small (<1 cm), and two other cases showed small, diffuse microcalcifications inside the lesion on CT. Delineation of mass edges was more easily appreciated on T1-weighted images with short TR (<550 ms) than on contrast enhanced CT.

The data yielded by both methods for fibrous and parasitic tissue were similar. Nevertheless, central necrosis and small peripheral cystic areas were more clearly identified on MR images (17 cases with MR and 15 with CT). One major flaw with MR was the lack of detectability of the clusters of microcalcification (four cases with MR but 17 cases with CT).

The topographic relationship between the parasitic lesions and hepatic veins or inferior vena cava were much better on MR than on CT images. Persistence of flow inside a hepatic vein or retro cava could be shown on MR in 13 cases but in only five cases on CT. Small cava thrombi were also well displayed in two cases. Portal vein involvement seemed to be equally well appreciated on MR images and on well opacified CT slices; analysis of portal branches in the left lobe was more difficult than in the right lobe because of the presence of artifacts in both methods. In one patient, disturbances of portal flow were shown by MR but not by CT (Fig. 5). Dilatation of biliary ducts (four cases) could be suspected from the MR data but it was more clearly seen on CT in every case. Extrahepatic extension was illustrated by both methods, but the sagittal and coronal views obtained by MR were helpful for a better analysis of the relationship between the parasitic mass and the vessels or diaphragm.

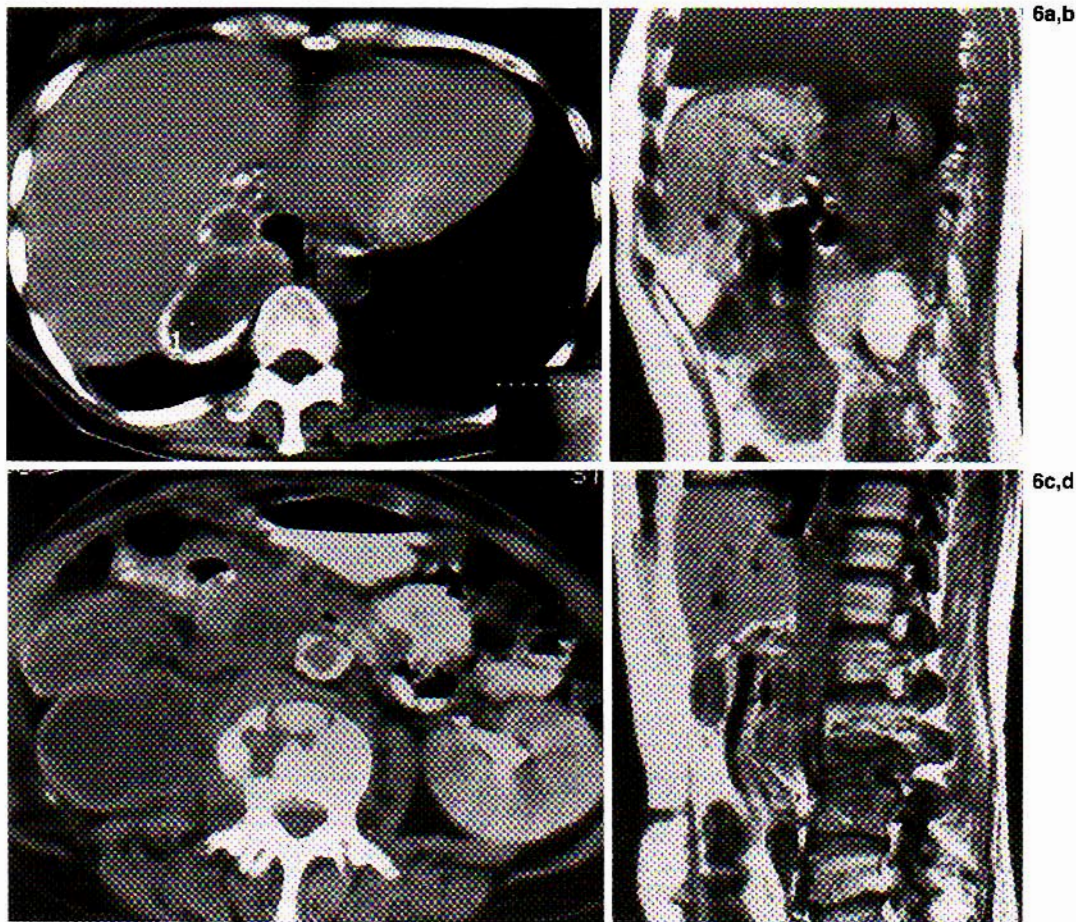


FIG. 6. Extrahepatic extension of a hepatic posterior mass. CT scan (a) and T1-weighted image (b) (with cardiac gating) show the transdiaphragmatic extension (arrow, b). CT scan (c) and T1-weighted image (d) (with cardiac gating) show retroperitoneal extension with involvement of the third and fourth lumbar vertebrae.

DISCUSSION

The comparison of MR and CT images with the classical pathological data (6) led to a clearer understanding of most of the MR patterns: (a) The fibrous and parasitic tissue showed a low signal on T1- and T2-weighted images in 15 of the 19 cases. This would appear to be due mainly to low proton density in the chronic fibroinflammatory reaction, containing small calcium deposits. This may be compared with the absence of enhancing after iodine injection in CT. In the other four cases a partial increase in signal on T2-weighted images may be observed near necrotic areas and may represent a pre-necrotic stage. In three cases small peripheral (<1 cm) round areas of high signal were shown at the periphery of the lesion. They may be due to peripheral parasitic cysts, the size of which may reach 10 mm (5). These peripheral cysts are better seen on MR than on CT and their diagnosis is important since they are thought to be the active part

of the lesion (6). (b) Massive necrosis has no characteristic appearance but seems to be more easily detected on MR than on CT. (c) Calcifications, especially in small clusters, are not readily seen on MR because of their very low signal, which is difficult to distinguish from fibrous and parasitic tissue.

In endemic areas AE is a challenge in the diagnosis of liver masses. The parasitic lesion is often discovered by ultrasound as a heterogeneous, mostly hyperechoic nonspecific mass, and by CT as a hypodense lesion without enhancement after iodine injection. The frequent presence of clusters of microcalcifications (90%) is of great value in establishing a positive diagnosis, especially if there are few clinical symptoms and/or suspicious history (e.g., rural life). This diagnosis, once suspected, can be easily confirmed by serological tests (4,5). In the past MR seemed to be of little interest since the small calcifications cannot be seen and no special pattern can be shown. Seven of nine of our cases

showed two or more foci, the mean size of which (3.5 cm) was smaller than in the cases of single foci (12.3 cm). This point emphasizes the utility of a complete pretherapeutic scanning to detect small lesions in other segments: even with T1-weighted images, MR did not detect several small lesions (diameter <2 cm). However, by comparison with the detection of metastases or small hepatocarcinoma, a further study with other MR pulse sequences will be useful to determine if the accuracy of MR can be improved.

The choice of treatment (medical therapy, hepatectomy, transplantation) is still under debate and depends on the degree of extension (2,9,10). The MR study at 0.5 T needs short TR spin echo T1-weighted images: the contrast between the lesion and normal liver is improved, and the delineation of mass edges and the study of vessels is easier. T2-weighted images are useful for the detection of small cystic peripheral extensions. Analysis of hepatic vein or vena cava extension is better with MR than CT and can differentiate between a deviation and an obstruction and detect a parasitic thrombi. Sonography is often inefficient in such cases because of the major attenuation of the ultrasound wave in the fibrous and parasitic mass (5). Magnetic resonance is also useful in showing transdiaphragmatic or retrohepatic extensions. Hence, MR is a necessary tool in the pretherapeutic evaluation of upper hepatic involvement. It may also be useful in the case of hilar extension or portal involvement, and in some cases of flow perturbations, which can be more easily shown than with CT.

The evolution of AE is very slow but capricious; in some cases, stability or only small internal modifications are observed over several years. There is no biological correlation, and radiological examinations are necessary for the follow-up of patients. Magnetic resonance is recommended for follow-up because of its precise delineation of lesion edges and vascular involvement; it does not require iodine

injection and avoids exposure to radiation. It will perhaps show changes in the appearance of the lesion during chemotherapy, as was described for hydatid cysts (11).

Acknowledgment: We thank Paul M. Walker for help in editing this paper and his technical criticisms in MR imaging.

REFERENCES

1. Thompson WM, Chisholm DP, Tank R. Plain film roentgenographic findings in alveolar hydatid disease—*Echinococcus multilocularis*. *Am J Roentgenol Radium Ther Nucl Med* 1972;116:345–58.
2. Kasai Y, Koshino I, Kawanishi N, Sakamoto H, Sasaki E, Kumagai M. Alveolar echinococcosis of the liver. Studies on 60 operated cases. *Ann Surg* 1980;191:145–52.
3. Maier W. Computed tomographic diagnosis of *Echinococcus alveolaris*. *Hepatogastroenterology* 1983;30:83–5.
4. Claudon M, Régent D, Delgoffe C, Bernard C, Gérard A, Tréheux A. Place de la scanographie dans le diagnostic et la surveillance de l'échinococcose alvéolaire hépatique. *J Radiol* 1985;66:507–13.
5. Didier D, Weiler S, Rohmer P, et al. Hepatic alveolar echinococcosis: correlative US and CT study. *Radiology* 1985;154:179–86.
6. Rauber G, Floquet J. Particularités morphologiques de l'échinococcose alvéolaire. *Lille Med* 1968;13:571–4.
7. Claudon M, Bracard S, Plenat F, Régent D, Bernadac P, Picard I. Spinal involvement in alveolar echinococcosis: assessment of two cases. *Radiology* 1987;162:571–2.
8. Gérard A, Canton P, Dureux JB. Treatment of alveolar echinococcosis with Albendazole (20 cases). In: *Recent advances in chemotherapy: proceedings of the 14th International Congress of Chemotherapy, Kyoto*. Tokyo: University of Tokyo Press. 1985: 2538–9.
9. Grosdidier J, Richaume B, Boissel P. Traitement chirurgical de l'échinococcose alvéolaire du foie. *Med Chir Dig* 1975;4:45–9.
10. Gillet M, Miguet JP, Manton G, et al. Orthotopic liver transplantation in alveolar echinococcosis of the liver: analysis of a series of six patients. *Transplant Proc* 1988;1:573–6.
11. Morris DL, Buckley J, Gregson R, Worthington BS. Magnetic resonance imaging in hydatid disease. *Clin Radiol* 1987;38:141–4.